Quantitative analysis of lower limb and pelvis deformities in children with X-linked hypophosphatemic rickets

Aurore **Bonnet-Lebrun**[1], Agnès **Linglart**[2,3], Marine **De Tienda**[1,4], Younes **Ouchrif**[1,4], Jugurtha **Berkenou**[3], Ayman **Assi**[5], Philippe **Wicart**[1,4], Wafa **Skalli**[1]

[1] Institut de Biomécanique Humaine Georges Charpak, Arts et Metiers ParisTech, 151 Boulevard de l'Hôpital, 75013 Paris, France

[2] APHP, Service d'endocrinologie pédiatrique, Hôpital Bicêtre Paris Sud, 94270 Le Kremlin-Bicêtre, France

[3] Centre de référence Maladies Rares du Métabolisme du Calcium et du Phosphore, 94270 Le Kremlin Bicetre, France

[4] APHP, Service d'orthopédie infantile, Hôpital Necker Enfants Malades, 75015 Paris, France

[5] Laboratoire de Biomécanique et d'Imagerie Médicale, Faculté de Médecine, Université de St Joseph, Beyrouth, Liban

Corresponding author:

A. Bonnet-Lebrun

Aurore.bonnet-lebrun@ensam.eu

Institut de Biomécanique Humaine Georges Charpak
151 Boulevard de l'Hôpital
75013 Paris, France

+33 6 75 13 23 85

Abstract

Introduction

X-linked hypophosphatemia (XLH) rickets mainly causes leg deformities in children that can get worse as they grow. We hypothesized that quantifying the bone parameters will help to document and monitor these deformities in children with XLH.

Methods

Thirty-five growing children affected by XLH were included in this cross-sectional study. Biplanar radiographs were taken with an EOS system allowing 3D reconstructions of the pelvis and legs. Sixteen geometric parameters were calculated for the legs and pelvis. A control group of 40 age-matched patients was used to define the reference values for these geometric parameters.

Results

For the legs, significant differences ($p < 0.05$) appeared between the XLH patients and the control group in the neck-shaft angle, femur/tibia length ratio and HKS. Among the 70 legs in the XLH group, 23 were in *genu varum*, 25 were in *genu valgum* and 22 were straight. There were significant differences between the *genu varum* and *genu valgum* subgroups in the femoral mechanical angle and the HKS. A strong correlation was found between the femoral mechanical angle and tibiofemoral angle ($r^2 = 0.73$) and between the femoral mechanical angle and HKS ($r^2=0.69$) The sacral slope and acetabular anteversion were significant different from the reference values.

Discussion

Quantitative radiological parameters derived from 3D reconstructions show that the deformities in XLH patients are 1) mainly in but not limited to the femoral shaft; 2) highly variable from one person to another. Some of these radiological parameters may be useful for the diagnosis and monitoring of XLH patients.

Level of evidence: III; Case control study

Mots clés : Enfant, Membres inférieurs, XLH, Déformations osseuses tridimensionnelles, Stéréoradiographie

Keywords: Child, Lower Extremity, XLH, Bone 3D Deformity, Biplanar Radiography

Introduction

X-linked hypophosphatemia (XLH) is one of the most common forms of hereditary rickets, with an incidence of about 1 per 20,000 births **[1-3]**. It primarily manifests itself by abnormal mineralization of bone and dental tissue **[1-3]**. Children affected by XLH have painful deformities of the legs, which are progressive and sometimes very severe **[2-3]**. These deformities appear when they start walking and can be partially corrected during growth with appropriate non-surgical treatment **[2-3]**. Once the growth phase has ended, only orthopedic surgery can improve the alignment of the lower limbs **[2-3]**; thus is it vital to have objective and quantitative information about these deformities and their progression during growth.

While several studies have been done on bone quality **[4-7]**, very few have focused on the bone geometry of the legs and pelvis in children with XLH. Bone deformity is currently evaluated by clinical measurement of intercondylar distances (ICD) and intermalleolar distances (IMD) and conventional 2D radiography **[2-5]**. This provides general information about the deformities, specifically in the frontal plane (*varus/valgu*s) and sagittal plane (*flessum/recurvatum)*. While the ICD and IMD measurements are useful for prospective monitoring by a clinician, they are not very reproducible **[3][8]**. Two scores have also been used to evaluate rickets on 2D radiographs. The Thacher score, developed for deficiency-related rickets, analyzes the alterations in the growth plate at the wrist and knees on a scale of 1 to 10 **[9]**. The "Radiographic Global Impression of Change", which is rated from –3 to +3, evaluates the deformity of the legs and progression of the rickets lesions between two radiographs taken at least 3 months apart **[7]**. But these two scores are not quantitative and are based on a subjective evaluation. Moreover, using 2D images to study complex three-dimensional (3D) deformities is subject to projection bias **[10-11]**.

The EOS® system (EOS Imaging, France) uses simultaneous biplanar acquisition to produce a personalized 3D model of the skeleton of a standing individual. This technique, which has been validated in adults and children **[10-13],** has been used to establish normality corridors for geometric parameters of the legs and pelvis in children of different age groups **[12-15]**. We hypothesized that quantifying the bone parameters will help to document and monitor these deformities in children with XLH.

The aim of this cross-sectional study was to characterize the deformities of the legs and pelvis in a population of children with XLH with the aim of identifying the radiological parameters that could be useful in the diagnosis or monitoring of patients.

Material and Methods

Patients

Thirty-five growing children with XLH, between 5 and 14.5 years of age were included in this cross-sectional study (**Table 1**); none had undergone surgery on their lower limbs. All were receiving non-surgical treatments. This study was approved by the local research ethics board (CPP06001) and consent was gathered from each patient and their parents. A control group, consisting of 40 asymptomatic age-matched children (20 girls, 20 boys), was used to define the reference values for the geometric parameters of the legs.

Radiographs & reconstructions

Radiographs of the entire body were made with the EOS® imaging system. Patients were placed in the standardized position defined by Chaibi et al. **[10]**: standing, right hallux at the level of the left plantar arch, hands on the mandible. A single trained operator did all the 3D reconstructions of the legs and pelvis using the improved Chaibi et al. method **[10][16]**: points of interest were selected by the operator, used to construct the first model which was back-projected on the AP/lateral radiographs, then adjusted by the operator until the contours of the back-projected model matched the image contours (**figure 1**).

Radiological parameters

From the 3D reconstruction, several parameters were calculated automatically (**table 2**, **figure 2**). For the pelvis, these parameters are the sacral slope, pelvic incidence and pelvic tilt **[12]** and for the acetabulum, these parameters are anteversion, coverage and inclination **[13]**.

For the legs, the parameters of interest are the femoral head diameter, femoral neck length, neck-shaft angle, femoral mechanical angle, tibial mechanical angle, tibiofemoral angle, angle between the mechanical axis and the femoral shaft (HKS), tibial and femoral anteversion, ratio of femoral length to tibial length **[14-15]**.

Statistical analysis

The leg and pelvis parameters from the children with XLH were compared to those of the control children with Student's *t*-test or the Wilcoxon-Mann-Whitney test, depending on whether the distribution was normal. The significance threshold was set at $p = 0.05$. The normality of the distributions was evaluated with the Lilliefors test.

To refine the analysis, the distribution of XLH patients in the normality corridor was calculated for each parameter. A normal value is one that falls within one standard deviation of the mean value of the control group. The value was subnormally high (low) when it was between +1 and +2 SD (−2 or −1 SD) and abnormally high (low) above this (below this).

Linear correlations between various parameters were determined by Pearson's method.

Lastly, the legs of the XLH patients were placed into three subgroups – *genu varum*, *genu valgum* and straight – based on the values of the tibiofemoral angle. The mean value of the control group was used as a reference **[15][17]**. The patients were classified as *genu varu*s when the tibiofemoral angle was greater than 1 SD of the mean of the control group, while it was *genu valgum* when lower. The parameters of the subgroup of patients with XLH and the control patients were compared with ANOVA or Kruskal-Wallis tests depending on their distribution.

Results

Figure 3 shows the wide range of deformities observed in children with XLH. Of note, certain patients have large femoral shaft curvatures, both in *varus/valgus* and in *flessum.*

Comparison with the normal range **[12-15]** is provided in **Table 3**. For the pelvis, 34% of acetabular anteversion values were abnormally low while 44% of sacral slope values were abnormally or subnormally high in patients with XLH. Statistical tests confirmed a significant difference between XLH and controls for these two parameters.

The main abnormalities in the lower limb were neck-shaft angle, ratio of femoral length to tibial length and tibial torsion with more than 35% of patients having abnormally low values, while 48% of patients had abnormally high HKS values. The diameter of the femoral head and neck length were not significantly different.

For parameters that were markedly different between the XLH patients and control, Figure 4 shows the distribution by age of the points corresponding to the legs of patients with XLH (n = 70) and the control group. There was a clear distinction between the two populations for the femur/tibia length ratio ($F/T_{mean,XLH} = 1.05$, $SD_{XLH} = 0.04$; $F/T_{mean,C} = 1.15$, $SD_C = 0.03$). The *genu varum* (n=23), *genu valgum* (n=25) and aligned (n=22) subgroups had significant differences in the tibiofemoral angle, femoral mechanical angle and HKS.

The correlation coefficient relating the femoral mechanical angle to the HKS and the femoral mechanical angle to the tibiofemoral angle was higher in the XLH patients than in the controls ($r^2 = 0.73$ versus $r^2 = 0.30$ and $r^2 = 0.69$ versus $r^2 = 0.21$, respectively) (**Figure 5**).

Discussion

The aim of this study was to define the bone deformities in the legs and pelvis of children with XLH rickets to identify relevant radiological parameters for their diagnosis and follow-up. We used 3D reconstructions to get around the projection bias related to 2D radiographs, particularly for complex 3D deformities like those induced by XLH **[10-11]**. Weightbearing radiographs allowed us to study positional parameters such as pelvic tilt along with morphological parameters **[11], [13], [16]**.

This cohort of 35 children with XLH rickets that is undergoing non-surgical treatment is representative of the current global population of children with XLH who are treated as soon as they are diagnosed **[2]**. The characteristics of this set of children, which is of comparable size to the largest study groups for this disease **[5]**, are consistent with what is expected from this pathology (**Table 1**) **[2]**, particularly in the 1/3 boy and 2/3 girl distribution.

Our study found a large diversity of 3D deformities in children with XLH, and hence, the benefit of characterizing each patient individually.

Several lower limb parameters, already studied in children in other pathological situations **[12-15]**, are modified because of XLH. In particular, parameters related to the femoral diaphysis such as the HKS, neck-shaft angle and femur/tibia length ratio are significantly different between the XLH patients and control children. This finding is consistent with existing qualitative studies **[3], [6]**. Conversely, the local parameters at the hip (femoral head diameter and neck length) do not appear to be affected. While no significant difference was found, likely because of the large variability even within the control group, tibial torsion appears reduced on average in XLH patients.

Looking at the *genu varum, genu valgum* and aligned subgroups and the correlation analysis revealed the predominant role of the femur in the tibiofemoral deformity in the frontal plane.

At the pelvis, the abnormalities were not as pronounced but still impacted the sacral slope and acetabular anteversion.

Based on this study, the most relevant markers to analyze the leg deformity in children with XLH at a given time are the femoral angles – femoral mechanical angle, neck-shaft angle and HKS – along with general parameters such as the femur/tibia length ratio and the tibiofemoral angle. Since the femoral mechanical angle appears to be correlated with the tibiofemoral angle and the HKS, calculating only the femoral mechanical angle, neck-shaft angle and femur/tibia length ratio appears to be sufficient to capture the main deformities in the legs. These highly reproducible markers **[10][15]**, could be incorporated in routine clinical and radiological evaluation of patients with XLH. The other radiological parameters presented in this article can refine the characterization of the deformity as needed.

These findings provide quantitative information about the bone deformities, but not allow us to evaluate the impact of these deformities on locomotion. A gait analysis of this population is currently underway.

Conclusion

Quantifying bone parameters in 3D revealed the nature of the deformities in children with XLH for the first time without projection bias. For all these patients, the deformities are mainly located in the femoral shaft, but not limited to it. Some of these radiological parameters may be useful for the diagnosis and monitoring of XLH patients. Moreover, the large range of deformities that exist in these XLH patients justifies characterizing each patient individually. By following these patients over several years, we will be able to quantify the effect of treatments on the changes in bone deformities during growth.

Conflict of interest

Professor Linglart received grants and fee reimbursement from Kyowa Kirin.

Professor Skalli has a patent related to the biplanar imaging system but does not personally receive any financial benefit from it.

Royalties from EOS Imaging are paid to the Georges Charpak Human Biomechanics Institute to fund research and education.

Funding

Kyowa Kirin Pharma provided financial support for this study.

Author contributions

A. Bonnet-Lebrun: study design, data acquisition and processing, writing of article

A. Linglart: study design, patient enrolment, scientific analysis, contributed to writing article

M. De Tienda, Y. Ouchrif: contributed to data acquisition and processing

J. Berkenou: patient enrolment, contributed to analyzing the clinical data

P. Wicart: study design, contributed to data acquisition, scientific analysis and writing the article

A. Assi: data from control subjects, contributed to data processing and scientific analysis

W. Skalli: study design, contributed to data processing, scientific analysis and writing the article

References

[1] Coyac BR, Falgayrac G, Penel G, Schmitt A., Schinke T, Linglart A, et al. Impaired mineral quality in dentin in X-linked hypophosphatemia. Connect Tissue Res. 2018;59:91–6

[2] Haffner D, Emma F, Eastwood DM, Biosse Duplan M, Bacchetta J, Schnabel D Wicart P et al. Clinical practice recommendations for the diagnosis and management of X-linked hypophosphataemia. Nat Rev Nephrol. 2019;15:435–55

[3] Gizard A, Rothenbuhler A, Pejin Z, Finidori G, Glorion C, Billy B, et al. Outcomes of orthopedic surgery in a cohort of 49 patients with X-linked hypophosphatemic rickets (XLHR). Endocr Connect. 2017;6:566–73

[4] Adams J. Radiology of Rickets ans Osteomalacia. 3rd ed. Vitamin D. 2011 chapter 49

[5] Lempicki M, Rothenbuhler A, Merzoug V, Franchi-Abella S, Chaussain C, Adamsbaum C, et al. Magnetic Resonance Imaging Features as Surrogate Markers of X-Linked Hypophosphatemic Rickets Activity. Horm Res Paediatr 2017;87:244-53

[6] Thacher T., Fischer P., and Pettifor J. The Effect of Nutritional Rickets on Bone Mineral Density. J Clin Endocrinol Metab 2014;99:4174-80

[7] Whyte M, Fujita K, Moseley S, Thompson D, and McAlister W. Validation of a Novel Scoring System for Changes in Skeletal Manifestations of Hypophosphatasia in Newborns, Infants, and Children: The Radiographic Global Impression of Change Scale. J Bone Miner Res, 2018;33:868-74

[8] Gupta P, Gupta V, Patil B, and Verma V. Angular deformities of lower limb in children: Correction for whom, when and how? J Clin Orthop Trauma 2020;11:196-201

[9] Thacher T, Fischer P, Pettifor J, Lawson J, Manaster B, and Reading J. Radiographic Scoring Method for Assessment of the Severity of Nutritional Rickets. J Trop Pediatr 2000;46:132-9

[10] Chaibi Y, Cresson T, Aubert B, Hausselle J, Neyret P, Hauger O, et al. Fast 3D reconstruction of the lower limb using a parametric model and statistical inferences and clinical measurements calculation from biplanar X-rays. Comput Methods Biomech Biomed Engin, 2012;15:457-66

[11] Gheno R, Nectoux E, Herbaux B, Baldisserotto M, Glock L, Cottea A, et al. Three-dimensional measurements of the lower extremity in children and adolescents using a low-dose biplanar X-ray device. Eur Radiol. 2012;22:765-71

[12] Mac-Thiong J-M, Labelle H, and Roussouly P. Pediatric sagittal alignment. Eur Spine J 2011;20:586-90

[13] Massaad A, Assi A, Bakouny Z, Sauret C, Kjallil N, Skalli W, et al. Three-dimensional evaluation of skeletal deformities of the pelvis and lower limbs in ambulant children with cerebral palsy. Gait Posture 2016;49:102-7

[14] Gaumétou E, Quijano S, Ilharreborde B, Presedo A, Thoreux P, Mazda K, et al. EOS analysis of lower extremity segmental torsion in children and young adults. Orthop Traumatol Surg Res, 2014;100:147-51

[15] Rampal V, Rohan P-Y, Assi A, Ghanem I, Rosello O, Simon A.-L, et al. Lower-limb lengths and angles in children older than six years: Reliability and reference values by EOS® stereoradiography. Orthop Traumatol Surg Res, 2018;104:389-95

[16] Quijano S, Serrurier A, Aubert B, Laporte S, Thoreux P, and Skalli W. Three-dimensional reconstruction of the lower limb from biplanar calibrated radiographs. Med Eng Phys, 2013;35:1703-12

[17] Salenius P, and Vankka E. The development of the tibiofemoral angle in children. J Bone Joint Surg Am. 1975;57:259-61

[18] Saraff V, Schneider J, Colleselli V, Ruepp M, Rauchenzauner M, Neururer S, et al. Sex-, age-, and height-specific reference curves for the 6-min walk test in healthy children and adolescents. Eur J Pediatr, 2015;174:837-40

Table 1: Patient characteristics

GENERAL PARAMETERS		
	Value (SD)	
Number	35	
Sex	23F/12M	
Age (years)	9.9 (2.3)	
Height (Z-score)	−0.48 (1.10)	
Growth rate, cm/year	6.7 (1.8)	
PHEX mutation	28 Yes /6 No /1 Unknown	
BMI (Z-score)	0.54 (0.89)	
Clinical laboratory		
	Value (SD)	Reference
ALP(1), IU/L	344 (122)	150-450
Phosphate(2) mmol/L	0.8 (0.2)	1.2-1.9
25 OH Vitamin D(1), ng/mL	38 (16)	30-80
PTH(1), ng/L	53 (25)	14-75
TRP(1), %	87 (11)	80-100
$6MWT_{ajusted}$(1) **[18]**, Z-score	−2.34 (1.08)	-

(1) at enrollment, (2) at diagnosis

SD: standard deviation, BMI: body mass index, ALP: alkaline phosphatase, PTH: parathormone, TRP: tubular reabsorption of phosphate, $6MWT_{adjusted}$: 6-minute walking test adjusted to age.

Table 2: Definition of parameters related to the pelvis **[14]** and the lower limbs **[12-13]**

Pelvis				
Type	*Name*	*Component 1*	*Component 2*	*Comment*
Angle	Sacral slope	Tangent to sacral growth plate	Horizontal	S_pelvis*
	Pelvic incidence	Vertical	Sacro-acetabular line**	S_pelvis*
	Pelvic tilt	Normal to sacral growth plate	Sacro-acetabular line**	S_pelvis*
	Acetabular anteversion	Frontal axis of pelvis projected on the sacral growth plate	Tangent line to acetabulum borders	Parallel plane to sacral growth plate
	Acetabular inclination	Normal to sacral growth plate	Normal to tangent plane to acetabular borders	
Ratio	Acetabular coverage	Surface of acetabulum	Sphere modeling the acetabulum	
Lower limbs				
Type	*Name*	*Component 1*	*Component 2*	*Comment*
Angle	Neck-shaft angle	Axis of superior diaphysis	Neck axis of femur	F_knee***
	Femoral mechanical angle	Femur's mechanical axis	Tangent to distal ends of condyles	F_knee*** Medial angle
	Tibial mechanical angle	Tibia's mechanical axis	Tangent to tibial plateau	F_knee*** Medial angle
	Tibiofemoral angle	Femur's mechanical axis	Tibia's mechanical axis	F_knee*** Lateral angle
	HKS	Axis of distal diaphysis	Femur's mechanical axis	
	Femoral torsion	Neck axis	Tangent posterior to condyles	Transverse plane of femur
	Tibial torsion	Tangent posterior to tibial plateaus	Bimalleolar axis	Transverse plane of tibia
Ratio	Femur/tibia	Length of femur between center of femoral head and trochlear groove	Length of tibia between the intercondylar eminence and pilon	
Length	Diameter of femoral head	Sphere modeling the femoral head		
	Length of neck	Defined between the center of the femoral head and intersection of the diaphyseal and neck axes		

* S_pelvis: sagittal plane of pelvis

** Joins the center of the sacral growth plate to a point in the middle of the two acetabulums

*** F_knee: frontal plane of knee

Table 3: Comparison to normality brackets for the pelvis **[12-13]** and lower limbs **[14-15]** of patients with XLH

	Abnormally low	Subnormally low	Normal	Subnormally high	Abnormally high
Pelvic parameters					
Sacral slope	5%	3%	49%	**30%**	**14%**
Incidence	0%	11%	62%	16%	11%
Version	3%	**35%**	41%	19%	3%
Acetabular parameters					
Anteversion	**34%**	23%	41%	3%	0%
Inclination	1%	5%	74%	16%	3%
Coverage	1%	18%	72%	9%	0%
Lower limb parameters					
Femoral torsion	**19%**	23%	39%	11%	9%
Tibial torsion	**36%**	24%	33%	4%	4%
Femoral mechanical angle	**28%**	9%	20%	10%	**34%**
Tibial mechanical angle	**23%**	16%	40%	13%	9%
Tibiofemoral angle	6%	8%	45%	18%	**24%**
Neck-shaft angle	**39%**	**38%**	23%	1%	0%
HKS	14%	10%	20%	9%	**48%**
Diameter of femoral head	0%	5%	69%	19%	8%
Length of neck	0%	5%	60%	33%	3%
Femur/tibia length ratio	**41%**	**36%**	23%	0%	0%

Distribution of patients with XLH into normal, subnormal and abnormal values

Note: in a normal asymptomatic population, 68% of values are normal, 27% are subnormal and 5% are abnormal.

Figure 1: Reconstruction of the lower limbs and pelvis using the method described by Chaibi et al. **[10]**

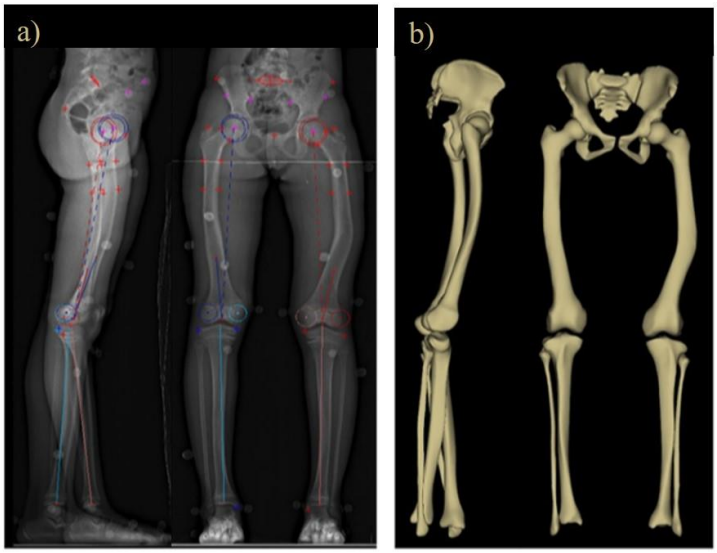

a) points selected, b) final model

Figure 2: Lower limb and pelvis parameters

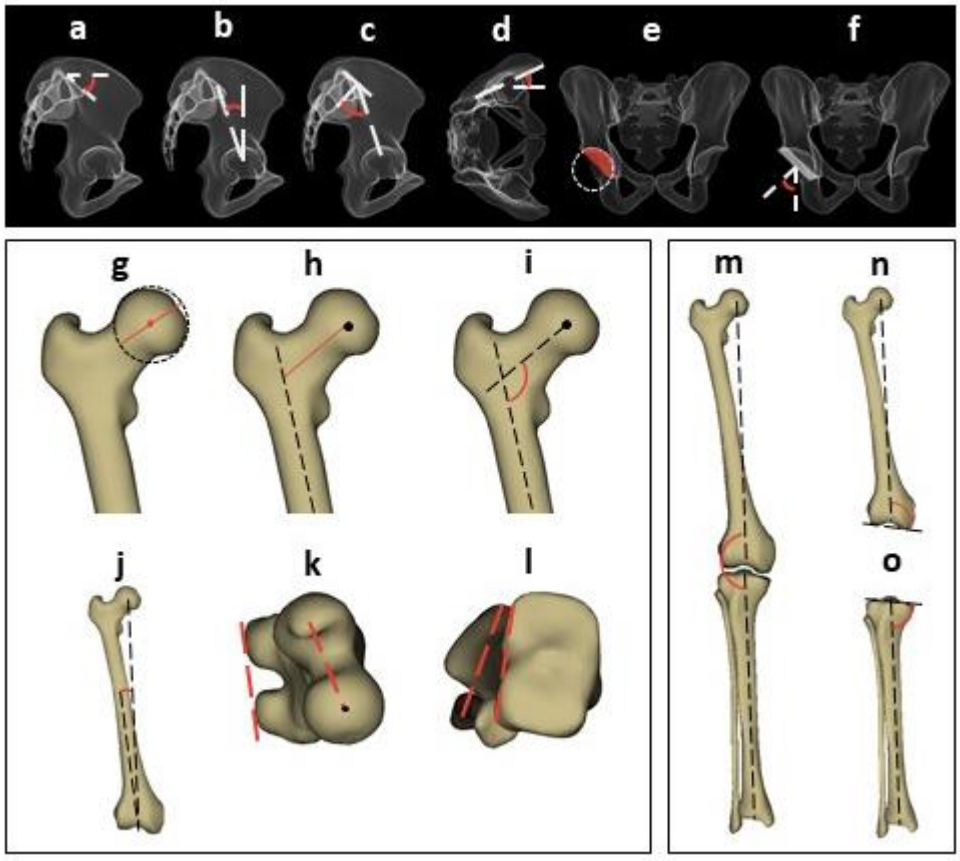

a) sacral slope, b) pelvic incidence, c) pelvic tilt, d) acetabular anteversion, e) acetabular coverage, f) acetabular inclination, g) diameter of femoral head, h) length of femoral neck, i) neck-shaft angle, j) HKS, k) femoral anteversion, l) tibial anteversion, m) tibiofemoral angle, n) femoral mechanical angle, o) tibial mechanical angle.

Figure 3: Example of the wide range of profiles found in this study

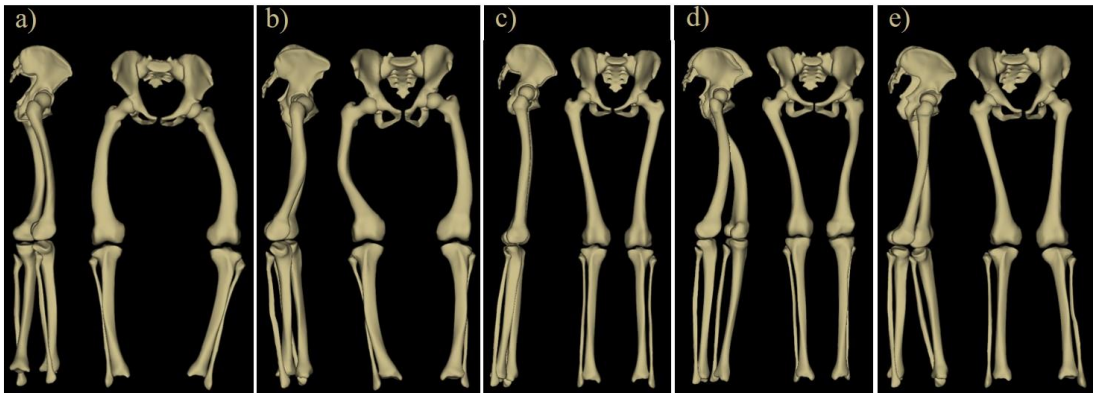

a) and b) deformity in varus, c) patient who is relatively symptomatic, d) and e) deformity in valgus.

Figure 4: Values of the lower limb parameters in the XLH population and the control group relative to age

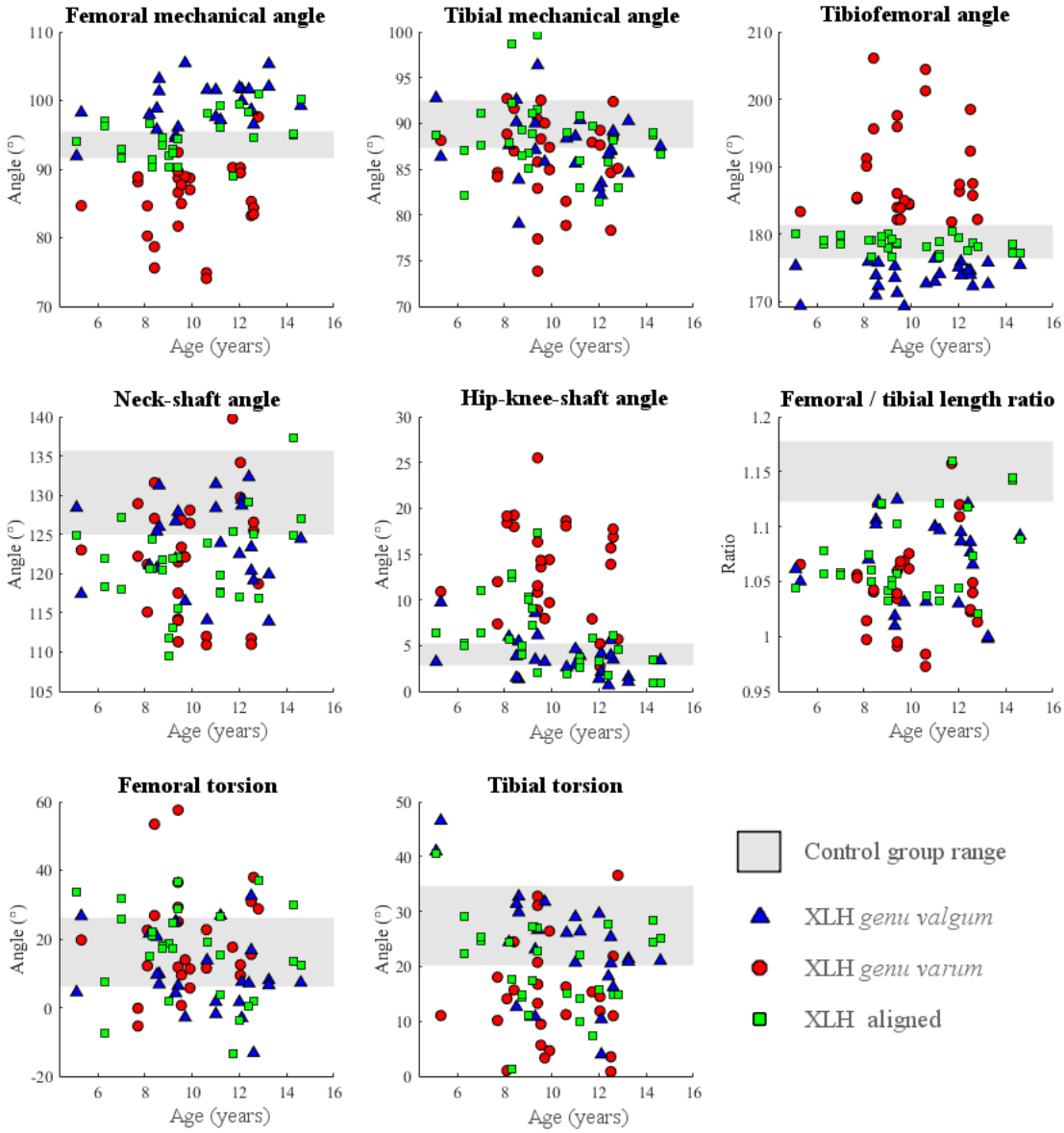

Figure 5: Correlation between the radiological parameters in children with XLH and asymptomatic controls.

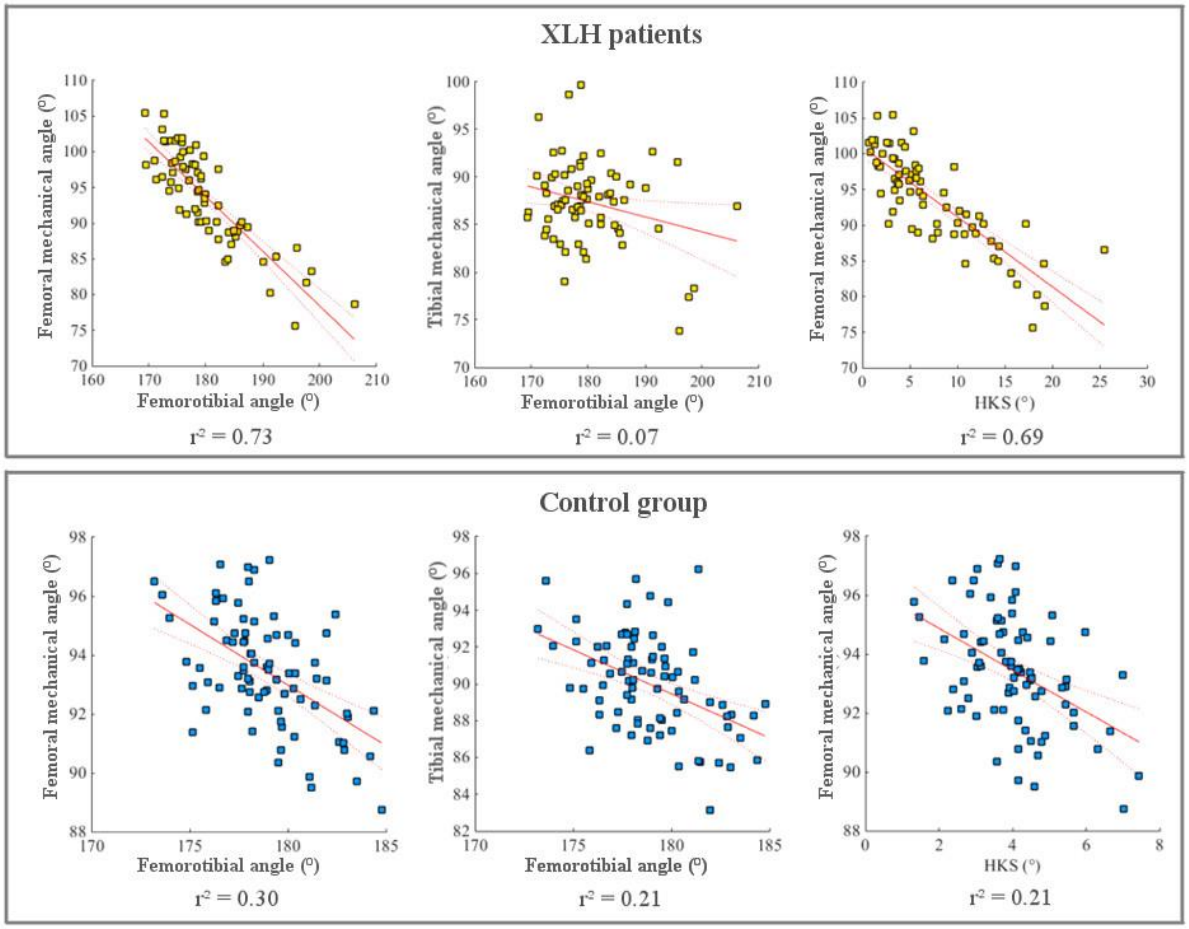

For each pair of parameters, the regression line, its confidence intervals and the square of the correlation coefficient are shown. The latter indicates how well the sample points match with the regression line.